On the Mechanism of Dehydration of a β-Hydroxycyclopentanone Analogue of Prostaglandin E_1

HYUK-KOO LEE *x, **HOWARD J. LAMBERT** ‡, and **RICHARD L. SCHOWEN** §

Received August 17, 1978, from the *Pharmacy R&D Department, Ayerst Laboratories, Rouses Point, NY 12979, the ‡Product Development Department, Searle Laboratories, Skokie, IL 60076, and the §Department of Chemistry, University of Kansas, Lawrence, KS 66045. Accepted for publication January 25, 1983.

Abstract □ The dehydration of the β-hydroxycyclopentanone, 11,16-dihydroxy-16-methyl-9-oxo-13-*trans*-protenoic acid methyl ester, an analogue of prostaglandin E_1, proceeds with acid catalysis (pH < 3), by uncatalyzed routes (pH ≃ 4 and ≃ 7), and with base catalysis (pH ≃ 5–6 and > 8). Deuterium from the solvent is not introduced α to the reactant keto function at 60% reaction at pH ≃ 1, but ~30% exchange has occurred at pH ≃ 5, 50% at pH ≃ 7, and 80% at pH ≃ 9. The data are consistent with a mechanism in which the substrate is initially enolized with catalysis by acid, base, and water to a 1,3-enediol, which looses water with catalysis by acid, base, and water. The first stage is rate determining in very acidic solution, while the second stage assumes the limitation of rate to an ever greater degree as the solution becomes more basic.

Keyphrases □ Prostaglandin E_1—β-hydroxycyclopentanone analogue, dehydration kinetics, mechanism □ Kinetics—dehydration of the β-hydroxycyclopentanone analogue of prostaglandin E_1, mechanism □ Dehydration—β-hydroxycyclopentanone analogue of prostaglandin E_1, mechanism, kinetics

The prostaglandins are a structural class of compounds exhibiting the most diverse biological activities (1). Prostaglandin E_1 (alprostadil, Ia) possesses, among other capacities, the potential for inhibiting gastric secretion in humans (2). The analogue of prostaglandin E_1 (Ib) also possesses this activity and is in fact 30-fold more potent than the parent compound when administered orally (3).

E-type prostaglandins tend to undergo dehydration to yield the unsaturated A (II) and B (III) forms (4–6) (Scheme I). We report here some observations on the dehydration of Ib, which illuminate the mechanistic character of its degradation.

EXPERIMENTAL

Materials—Racemic mixtures of the 16α- and 16β-hydroxy epimers and their respective antipodes for 11,16-dihydroxy-16-methyl-9-oxo-13-*trans*-protenoic acid methyl ester (Ib, SC-29333) and its dehydration products, IIb and IIIb, were used as supplied[1].

Kinetics—The UV assay method developed by Monkhouse *et al.* (5) was adopted to follow the dehydration kinetics of Ib. Stock solutions of Ib (2.53×10^{-3} M in methanol) were diluted 50-fold with thermostated aqueous buffer (glycine–HCl, acetic acid–sodium acetate, sodium dihydrogen phosphate–sodium hydroxide, boric acid–sodium hydroxide), purged with nitrogen, and maintained at a constant temperature. Samples were withdrawn at measured intervals and spectra were recorded in Suprasil cells[2] from 200–350 nm. First-order rate constants were calculated; the pH values of the highly acidic solutions were calculated from the known concentrations of hydrochloric acid, with mean activity coefficients obtained or extrapolated from literature data (7). The pH values of the buffer solutions were read at the temperature of study with a pH-meter[3] standardized at the same temperature.

Deuterium Exchange—Exchange reactions were carried out to ~60% dehydration under each set of conditions, in a 44% (v/v) deuterated methanol–deuterated water solvent (CD_3OD–D_2O) of 4.5-mL volume, containing 20 mg of Ib. This solution was then extracted with 5 mL of $CDCl_3$; the extract was evaporated under nitrogen and reconstituted to 3 mL with $CDCl_3$. The NMR spectrum at 350–500 Hz downfield from tetramethylsilane was recorded with 150-Hz scale expansion and time averaging. The ratio of integrated peak areas for the α-H at C-10 (368 Hz) to that of the β-H at C-11 (448 Hz) was calculated.

Experiments were initiated by combining 2 mL of a CD_3OD solution of Ib with 2.5 mL of a D_2O solution of appropriate materials. The latter solutions were: (*a*) 0.1 M DCl in D_2O; (*b*) 29 mg of CH_3COONa and 0.1 mL of CD_3COOD in 10 mL of D_2O; (*c*) 68 mg of KH_2PO_4 and 1.49 mL of 0.2 M NaOD in 10 mL of D_2O; and (*d*) 31 mg of H_3BO_3 and 4.4 mL of 0.1 M NaOD in 10 mL of D_2O. The corresponding temperature and reaction times were: (*a*) 60°C, 3.5 h; (*b*) 70°C, 113 h; (*c*) 80°C, 6 h; and (*d*) 50°C, 2 h.

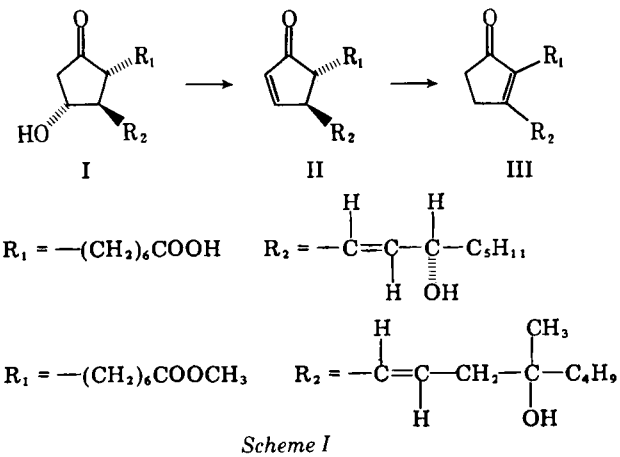

Scheme I

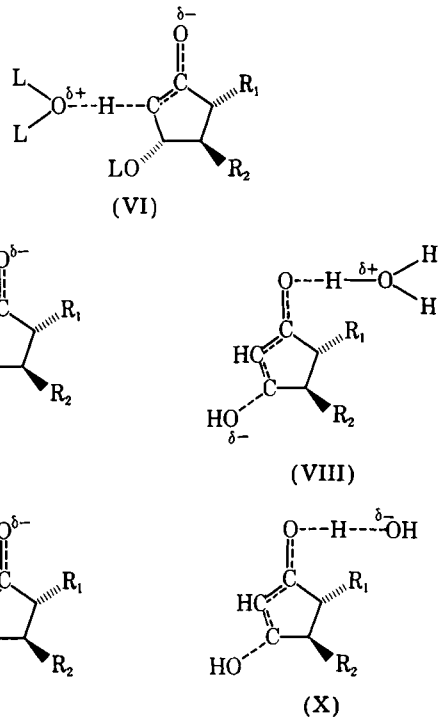

[1] Ib, IIb, and IIIb were provided by the Chemical Development and Chemical Research Departments of Searle Laboratories.
[2] Suprasil Cell; Scientific Products, McGaw Park, Ill.
[3] pH-Meter; Radiometer, Copenhagen, Denmark.

0022-3549/84/0300-0306$01.00/0

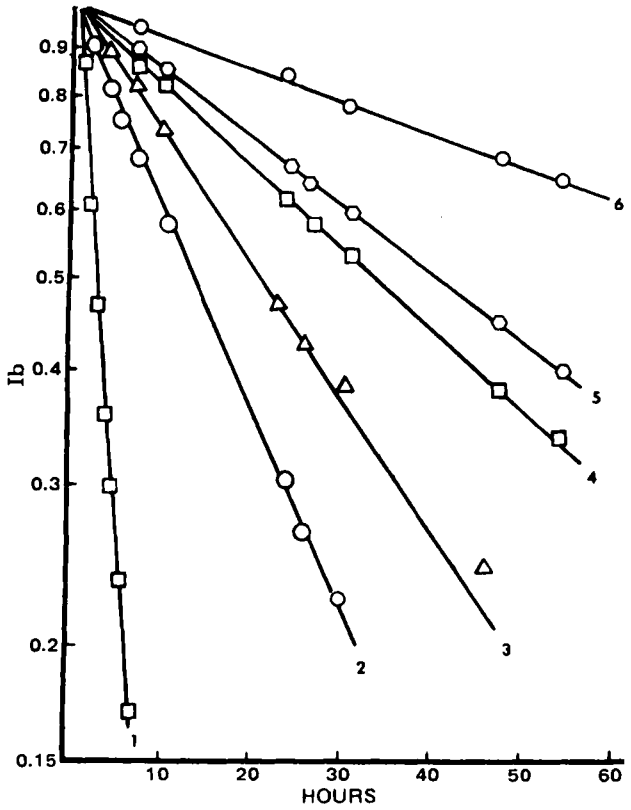

Figure 1—*Typical apparent first-order plots for the dehydration reaction of Ib at 60°C. Key: (1) 0.1 M HCl, pH 1.11; (2) 2.60 × 10^{-3} M KH_2PO_4-NaOH, pH 7.65; (3) 3.18 × 10^{-3} M KH_2PO_4-NaOH, pH 7.23; (4) 2.60 × 10^{-3} M KH_2PO_4-NaOH, pH 6.72; (5) 3.30 × 10^{-3} M KH_2PO_4-NaOH, pH 6.24; (6) 1.6 × 10^{-3} M CH_3COOH-CH_3COONa, pH 5.14.*

Solvent Isotope Effect—The solvent isotope effect in acidic solution was monitored at 80°C. This study utilized 0.01 M HCl (pH 2.0) with 1% methanol and ~0.01 M DCl (pD was adjusted to 2.0) with 1% CD_3OD.

RESULTS AND DISCUSSION

Stoichiometry—The dehydration of Ib was followed by the appearance of UV bands characteristic of IIb (λ_{max} 222 nm, ϵ 11,000) and IIIb (λ_{max} 288, ϵ 28,000), as shown by independent synthesis and spectral study of IIb and IIIb. Compound IIb appeared to be formed first and then converted to IIIb, which also decreased in concentration after some time. Small amounts of other products, including the 8-epimers of Ib and IIb, could be detected by HPLC, but were minor (<10%) in comparison with IIb and IIIb in 0.1 M HCl and pH 7.4 solutions at 60°C. It is very unlikely that the 8-epimer formation affects the rate of the dehydration reaction of Ib (I → II).

Another possible reaction intermediate, a prostaglandin C-type product (IV), could be formed (Scheme II). Jones (8) reported that prostaglandin C in methanol exhibits a UV λ_{max} at 234 nm (ϵ 21,000) with shoulders occurring at 228 and 243 nm. However, there was no indication of formation of this type of intermediate in the UV spectra throughout the course of the present kinetic studies. It may, of course, be formed but not accumulated in sufficient amounts to be detected because of the instability of this intermediate (8, 9).

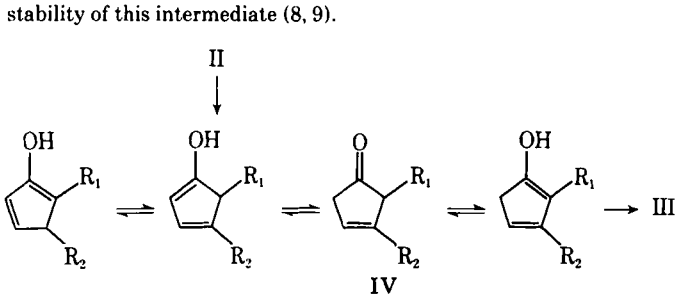

Scheme II

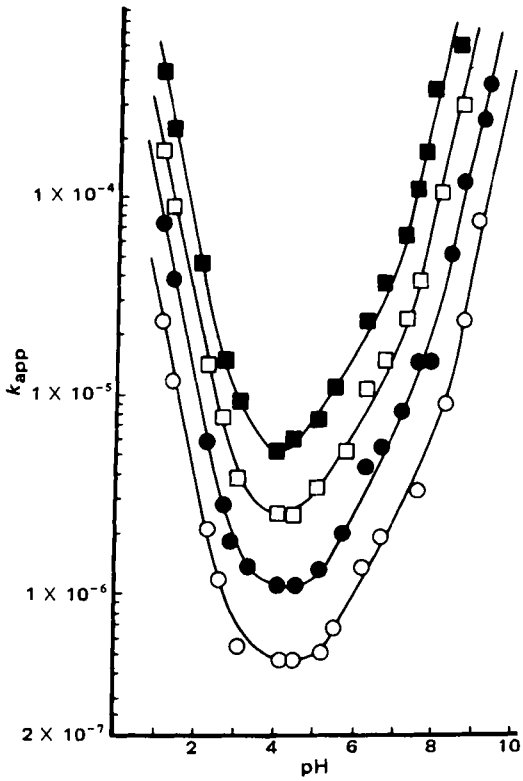

Figure 2—*Log k_{app}-pH profiles for the dehydration kinetics of Ib at several temperatures, where all points were experimentally obtained and the solid lines were fitted by Eq. 1. Key: (○) 50°C; (●) 60°C; (□) 70°C; (■) 80°C.*

When the concentration of Ib at any time was calculated from [Ib] = $[Ib]_0$ − ([IIb] + [IIIb]), with [IIb] and [IIIb] determined spectrophotometrically, first-order plots for loss of Ib were linear for two or more half-lives. Typical first-order plots at various pH values are given in Fig. 1. These data suggest that the major process under study is the irreversible conversion of Ib to IIb, which then proceeds to IIIb and other materials (Scheme I). Our observations do not bear on the conversion of IIb to IIIb or other products, although it is easy to see how IIIb might form from IIb by two simple proton-transfer reactions.

Effect of pH—The complete log k_{app}-pH profiles for the dehydration reaction of Ib at four temperatures are given in Fig. 2. Buffers were used to maintain the pH, but at a concentration of only 3 × 10^{-3} M so that the effects are essentially those of pH. The points of Fig. 2 are experimental; the lines are theoretical and are derived from:

$$k_{app} = k_H a_H + k_0 + k_B \frac{K_a}{K_a + a_H} + k_{OH} \frac{K_w}{a_H} \qquad \text{(Eq. 1)}$$

The rate constants k_H, k_0, k_B, and k_{OH}, as well as the apparent dissociation constant K_a, were shown to be a complex combination of rate constants (no simple definition of those empirical constants can reliably be made at the present stage; however, see Eqs. 13–17). These constant values were determined from the best fit of the log k_{app}-pH profiles in accordance with Eq. 1 (Table I).

Activation Parameters—The Arrhenius plots for the rate constants of Eq. 1 are shown in Fig. 3. The enthalpies and entropies of activation

Table I—Apparent Catalytic Rate Constants (k_H, k_0, k_B, and k_{OH}) and Kinetic Dissociation Constant (K_a) for the Dehydration of Ib in Aqueous Solution (1% Methanol) at Various Temperatures [a]

Temperature, °C	$k_H \times 10^3$, $M^{-1}\cdot s^{-1}$	$k_0 \times 10^6$, s^{-1}	$k_B \times 10^5$, s^{-1}	k_{OH}, $M^{-1}\cdot s^{-1}$	$K_a \times 10^6$, M
50 ± 0.5	0.29	0.46	0.03	0.69	0.21
60 ± 0.5	0.94	1.11	0.57	1.55	0.27
70 ± 0.5	2.16	2.47	0.75	4.27	1.27
80 ± 0.5	5.74	5.20	1.11	9.44	3.59

[a] Determined from the best fit of the log k_{app}-pH profiles in accordance with Eq. 1.

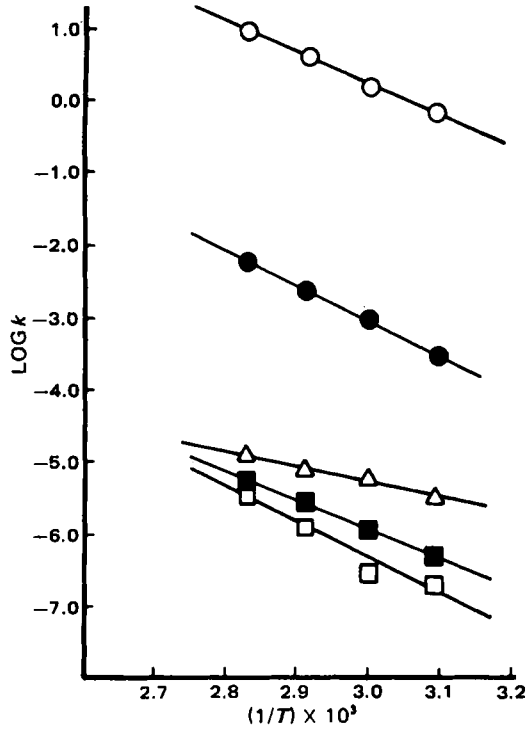

Figure 3—*Arrhenius plots for the apparent catalytic rate constants and the kinetic dissociation constant of dehydration kinetics of I, where each constant was defined by Eqs. 13–17 and each unit was shown as in Table I. Key:* (○) k_{OH}; (●) k_H; (△) k_B; (■) k_0; (□) K_a.

for each constant of Eq. 1 are shown in Table II.

Solvent Isotope Effect—At 80°C and pH (pD) 2.0, the ratio $k_H(H_2O)/k_H(D_2O)$ was found to be 0.8.

Deuterium Exchange at C-10 of Ib—It was possible to make an approximate determination of the degree of deuterium incorporation at the methylene carbon next to the keto function of Ib (C-10) by comparing the intensity of the NMR signal for the α-hydrogen at C-10 (368 Hz) to that of the β-hydrogen at C-11 (448 Hz). The NMR spectrum of IIb obtained from the dehydration reaction of Ib in a medium of 0.05 M DCl–45% CD_3OD showed that no incorporation occurred up to 60% reaction at 60°C. In deuterated acetate buffer in the same solvent at 70°C, ~30% of the C-10 hydrogen had been exchanged at 60°C reaction. A similar experiment with deuterated phosphate buffer showed 50% exchange at 80°C and with deuterated borate buffer 80% exchange at 50°C.

General base catalysis of enolization by buffers might give a larger ratio of exchange to dehydration at the higher buffer concentrations used in the exchange experiments in comparison with the kinetic experiments. However, it seems very unlikely that it could have resulted in an incorrect assignment of the rate-determining steps, since enolization seems clearly established as rate determining at low pH and the shape of the pH–rate profiles requires a partial change in the rate-determining step at pH >7 (*cf., Mechanistic Analysis*).

Formulation of the Rate Equation—A simple mechanism for loss of I, consistent with these findings, is shown in Scheme III. This postulates the conversion of I to its enolic form (V), which is assumed to be present in low steady-state concentrations, by pathways involving acid, base, and water catalysis (10). The enol V then decomposes by three similar pathways to II. Of course, V will be partly or wholly converted to enolate in the more basic solutions, but this will not affect the observable

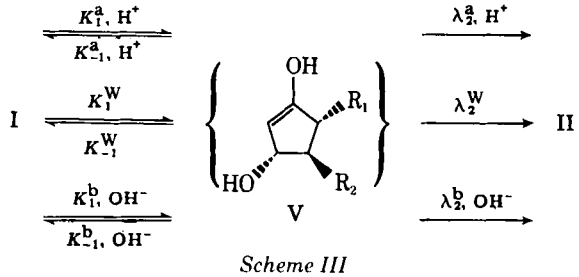

Scheme III

Table II—Activation Parameters[a] Associated with the Catalytic Constants for the Dehydration of Ib

Catalytic Constant[b]	$\Delta H^{\ddagger}$, kcal/mol	$\Delta S^{\ddagger}$, cal/K·mol
k_H	22 ± 1	−7 ± 3
k_0	18 ± 1	−31 ± 3
k_B	10 ± 1	−54 ± 3
k_{OH}	20 ± 1	+2 ● 3
K_a	19 ± 2[c]	+29 ± 6[c]

[a] Standard states of unit molarity at 80°C. [b] See Eq. 1. [c] These are properly $\Delta H°$ and $\Delta S°$ for interconversion of activated complexes.

kinetics (and cannot be deduced from the kinetics, only assumed on the basis of analogy).

In Scheme III, k_1^a, k_1^w, and k_1^b are the rate constants for hydronium ion-, neutral (water), and hydroxide ion-catalyzed enolization. The terms k_{-1}^a, k_{-1}^w, and k_{-1}^b are for the reverse enolization reaction. For dehydration, λ_2^a, λ_2^w, and λ_2^b are the rate constants for the hydronium ion-, neutral (water), and hydroxide ion-catalyzed dehydration reaction (V → II).

The rate of change in concentration of I, II, and V is described by:

$$-\frac{d[I]}{dt} = (k_1^a a_H + k_1^w + k_1^b K_w/a_H)[I] - (k_{-1}^a a_H + k_{-1}^w + k_{-1}^b K_w/a_H)[V] \quad \text{(Eq. 2)}$$

$$\frac{d[V]}{dt} = (k_1^a a_H + k_1^w + k_1^b K_w/a_H)[I] - (k_{-1}^a a_H + k_{-1}^w + k_{-1}^b K_w/a_H)[V] - (\lambda_2^a a_H + \lambda_2^w + \lambda_2^b K_w/a_H)[V] \quad \text{(Eq. 3)}$$

The steady-state kinetic law for this mechanism is:

$$k_{app} = \frac{(k_1^a a_H + k_1^w + k_1^b K_w/a_H)(\lambda_2^a a_H + \lambda_2^w + \lambda_2^b K_w/a_H)}{k_{-1}^a a_H + k_{-1}^w + k_{-1}^b K_w/a_H + \lambda_2^a a_H + \lambda_2^w + \lambda_2^b K_w/a_H} \quad \text{(Eq. 4)}$$

It is convenient to multiply the numerator and denominator of Eq. 4 by the equilibrium constant (K_1) for enolization of I:

$$K_1 = (k_1^a/k_{-1}^a) = (k_1^w/k_{-1}^w) = (k_1^b/k_{-1}^b) \quad \text{(Eq. 5)}$$

This yields Eq. 6, in which $k_2^a = K_1\lambda_2^a$, $k_2^w = K_1\lambda_2^w$, and $k_2^b = K_1\lambda_2^b$:

$$k_{app} = \frac{(k_1^a a_H + k_1^w + k_1^b K_w/a_H)(k_2^a a_H + k_2^w + k_2^b K_w/a_H)}{(k_1^a + k_2^a)a_H + (k_1^w + k_2^w) + (k_1^b + k_2^b)K_w/a_H} \quad \text{(Eq. 6)}$$

This formulation has the advantage that each rate constant has an initial reference state of I, rather than some referring to I (the K values) and some to V.

The mechanistic kinetic law of Eq. 6 can be related to the phenomenological law of Eq. 1 by expanding the numerator of Eq. 6. Each term in the expansion will be important in a particular pH region:

1. In acidic solution, only terms in a_H are important, and so Eq. 6 can be simplified to:

$$k_{app} \cong \frac{k_1^a k_2^a}{(k_1^a + k_2^a)} a_H \quad \text{(Eq. 7)}$$

2. In less acidic conditions (pH ~4), only k_1^w and k_2^w may be important, so that:

$$k_{app} \cong \frac{k_1^w k_2^w}{(k_1^w + k_2^w)} \quad \text{(Eq. 8)}$$

3. Near neutral pH, acid-catalytic terms are not important, so that:

$$k_{app} \cong \frac{k_1^w k_2^w (a_H)^2 + k_1^b k_2^b (K_w)^2 + k_1^w k_2^b K_w a_H + k_1^b k_2^w K_w a_H}{[(k_1^w + k_2^w)a_H + (k_1^b + k_2^b)K_w]a_H} \quad \text{(Eq. 9)}$$

where $k_1^w k_2^w (a_H)^2$ and $k_1^b k_2^b (K_w)^2$ are negligible, so that Eq. 9 gives:

$$k_{app} \cong \left(\frac{k_1^b k_2^w + k_2^b k_1^w}{k_1^b + k_2^b}\right) \frac{\left[\frac{(k_1^b + k_2^b)K_w}{k_1^w + k_2^w}\right]}{\left[\frac{(k_1^b + k_2^b)K_w}{k_1^w + k_2^w}\right] + a_H} \quad \text{(Eq. 10)}$$

4. At high pH (pH >9) only the k_1^b and k_2^b are important, so that Eq. 6 is simplified to:

$$k_{app} \cong \frac{k_1^b k_2^b}{(k_1^b + k_2^b)}\left(\frac{K_w}{a_H}\right) \quad \text{(Eq. 11)}$$

The overall rate expression, k_{app}, may be represented as the sum of Eqs. 7, 8, 10, and 11, because when one term is important, all the others are not:

$$k_{app} \cong \left(\frac{k_1^a k_2^a}{k_1^a + k_2^a}\right) a_H + \left(\frac{k_1^w k_2^w}{k_1^w + k_2^w}\right) + \left(\frac{k_1^b k_2^w + k_1^w k_2^b}{k_1^b + k_2^b}\right) \cdot \frac{\left[\frac{(k_1^b + k_2^b)K_w}{k_1^w + k_2^w}\right]}{\left[\frac{(k_1^b + k_2^b)K_w}{k_1^w + k_2^w}\right] + a_H} + \left(\frac{k_1^b k_2^b}{k_1^b + k_2^b}\right) \cdot \frac{K_w}{a_H} \quad \text{(Eq. 12)}$$

A comparison of Eqs. 1 and 12 reveals that both have the same mathematical form, so that Eq. 11 provides the correct log k_{app}–pH profiles for the dehydration of I. From Eqs. 1 and 12, the relationships shown in Eqs. 13–17 are obtained:

$$k_H = \frac{k_1^a k_2^a}{k_1^a + k_2^a} \quad \text{(Eq. 13)}$$

$$k_0 = \frac{k_1^w k_2^w}{k_1^w + k_2^w} \quad \text{(Eq. 14)}$$

$$k_B = \frac{k_1^b k_2^w + k_1^w k_2^b}{k_1^b + k_2^b} \quad \text{(Eq. 15)}$$

$$k_{OH} = \frac{k_1^b k_2^b}{k_1^b + k_2^b} \quad \text{(Eq. 16)}$$

$$K_a = \frac{(k_1^b + k_2^b)K_w}{k_1^w + k_2^w} \quad \text{(Eq. 17)}$$

Mechanistic Analysis—The deuterium exchange data and solvent isotope effect can aid in bringing out further detail. First, at low pH, as Eq. 13 emphasizes, either hydronium-catalyzed proton removal from I (k_1^a) or hydronium-catalyzed elimination of water from V (k_2^a) determines the rate. Lack of deuterium exchange suggests that $k_2^a > k_1^a$ (no reversion from V), so that $k_{app} \simeq k_1^a a_H$, with a rate-limiting transition state resembling VI (where L = H in H_2O, D in D_2O).

The solvent isotope effect at 25°C for such a transition state would be given (11) by $k_{H_2O}/k_{D_2O} = (0.69)^3/\phi_1\phi_2^2$, where ϕ_1 and ϕ_2 are isotopic fractionation factors relative to water for the hydrogen attached to the keto group (ϕ_1) and those of the reacting water molecule (ϕ_2). For a limiting reactant-like structure, $\phi_1 \sim 0.69$, $\phi_2 \sim 1.0$ and $k_{H_2O}/k_{D_2O} = 0.48$. For a limiting product-like structure, $\phi_1 \sim 1.0$, $\phi_2 \sim 0.69$, and $k_{H_2O}/k_{D_2O} = 0.69$. Rough correction to 80°C gives limiting predictions of 0.53 (reactant-like) and 0.73 (product-like). The latter is not far from the observed effect of 0.8 ± 0.1.

In acetate buffer, exchange of deuterium concurrently with reaction was observed, with ~30% exchange accompanying 60% dehydration. In this pH range, the dominant term is k_0 (Eq. 14). The exchange indicates some reversion from enol to reactant, so that apparently $k_2^w \gtrsim k_1^w$, with enol formation more important than elimination but not exclusively rate determining ($k_{app} \simeq k_1^w$).

Setting aside the phosphate buffer experiment momentarily, we can examine the borate buffer findings. These pertain to the high pH region governed by k_{OH} (Eq. 16). Since exchange exceeds dehydration (80% exchange, 60% dehydration), base-catalyzed decomposition of the enol dominates but does not wholly control rate limitation ($k_1^b \gtrsim k_2^b$, $k_{app} \simeq k_2^b K_w/a_H$).

Returning to the phosphate buffer exchange data, we note that these are related to the pH region of ~7, where:

$$k_{app} = k_B \frac{K_a}{K_a + a_H} \quad \text{(Eq. 18)}$$

with k_B given by Eq. 15 and K_a by Eq. 17. At low pH in this range, $k_{app} \simeq k_B K_a/a_H$ or:

$$k_{app} = \frac{(k_1^b k_2^w + k_1^w k_2^b)K_w}{(k_1^w + k_2^w)a_H} \quad \text{(Eq. 19)}$$

From arguments in the last two paragraphs, $k_1^b \gtrsim k_2^b$ and $k_2^w \gtrsim k_1^w$, so we can expect that $k_1^b k_2^w > k_1^w k_2^b$ in Eq. 19, or:

$$k_{app} = \frac{(k_1^b k_2^w)K_w}{(k_1^w + k_2^w)a_H} \simeq k_1^b K_w/a_H \quad \text{(Eq. 20)}$$

so that the main rate-limiting process at the acidic end of this pH range is base-catalyzed enolization (presumably proton abstraction from I by the hydroxide ion). At the high pH end of the range, $k_{app} \simeq k_B$ (*cf.* Eq. 15), and by the same arguments as just given:

$$k_{app} \simeq \frac{k_1^b k_2^w}{k_1^b + k_2^b} \simeq k_2^w \quad \text{(Eq. 21)}$$

so that the rate-determining step now tends toward water-catalyzed elimination from V. If enol formation truly determined the rate below pH 7, no exchange would be expected there, and if elimination from the enol truly determined the rate above pH ~7, then 100% exchange would be expected there. In fact, in a phosphate buffer, ~50% exchange was observed at 60% reaction.

We can compare finally the deductions made from the kinetics and the exchange experiments with the activation parameters for consistency. For example, we conclude that k_H is dominated by k_1^a with a transition-state structure like VI. From Table II, the formation of VI from I and hydronium ion is indicated to require $\Delta H^\ddagger \simeq 22$ kcal/mol, $\Delta S^\ddagger \simeq -7$ eu. These are acceptable in terms of the hypothesis, a small negative $\Delta S^\ddagger$ being consistent with a bimolecular process in which some solvation (presumably from the hydronium ion) is released.

For the region of pH 4–5 where k_0 rules, the most important rate constant was k_1^w with some contribution from k_2^w. Speculative structures for the transition state would be VII and VIII, respectively. According to Table II, conversion of I in aqueous solution to chiefly VII and some VIII is accompanied by $\Delta H^\ddagger = 18$ kcal/mol, $\Delta S^\ddagger = -31$ eu. The entropy change, in particular, is reasonable for the "freezing" of water molecules associated with proton transfer and development of change. Since k_B is roughly determined by k_2^w (see argument for Eq. 21), its activation parameters should also correspond to those expected for a transition state like VIII. Indeed the values found ($\Delta H^\ddagger = 10$ kcal/mol, $\Delta S^\ddagger = -54$ eu) are of the magnitudes anticipated.

For k_{OH}, determined chiefly by k_2^b with some contribution from k_1^b, the appropriate transition-state structures are IX and X. Here, as for formation of VI, the energy-requiring, entropy-producing release of water on binding of the strongly solvated hydroxide ion to generate a charge-delocalized transition state leads to relatively large $\Delta H^\ddagger$ (20 kcal/mol) and—from compensation with entropy loss in the bimolecular reaction—to a negligible $\Delta S^\ddagger$ (2 eu).

Lastly we have the equilibrium constant K_a, defined by Eq. 17. This equilibrium constant is for the reaction of Eq. 22; the reactant state for this equilibrium:

$$\begin{Bmatrix} \text{VII} \\ \text{VIII} \end{Bmatrix} \rightarrow H^+ + \begin{Bmatrix} \text{IX} \\ \text{X} \end{Bmatrix} \quad \text{(Eq. 22)}$$

is a weighted average of activated complexes VII and VIII (for water-catalyzed enolization and elimination, respectively), the more stable transition state contributing more to the average, while the product state is a similar weighted average of IX and X (for base-catalyzed formation and decomposition of enol). As the values of K_a in Table I show, the water-catalysis activated complexes are acids of $pK_a \simeq 5.4$–6.7 at 50–80°C, with pK_a estimated at 7.6 at 25°C. As anticipated, this is intermediate between values of 1.74 for H_3O^+ (product-like structure for VII–X) and 15.74 (reactant-like structure for VII–X).

On the other hand, the thermodynamic parameters of ionization are unlike those of stable acids, as judged by the very extensive collection of Izatt and Christensen (12). Most stable acids have smaller, positive ΔH (compared with 19 kcal/mol) and much more negative ΔS (*versus* 29 eu) of ionization than these activated complexes. Conceivably this is a reflection of a greater internal structural plasticity of activated complexes and the greater attendant release of solvation upon ionization.

REFERENCES

(1) T. K. Schaaf, *Annu. Rep. Med. Chem.*, **11**, 80 (1976).

(2) M. Classen, H. Koch, J. Bickhart, G. Topf, and L. Demling, *Digestion*, **4**, 333 (1971).

(3) E. Z. Dajemi, D. R. Driskill, R. G. Bianchi, P. W. Collins, and R. Pappo, *Digest. Dis.*, **21**, 1049 (1976).

(4) N. H. Andersen, *J. Lipid Res.*, **10**, 320 (1969).

(5) D. C. Monkhouse, L. Van Campen, and A. J. Aguiar, *J. Pharm. Sci.*, **62**, 576 (1973).

(6) G. F. Thompson, J. M. Collins, and L. Schmalzried, *J. Pharm. Sci.*, **62**, 1738 (1973).

(7) H. S. Harned and B. B. Owens, "The Physical Chemistry of Electrolytic Solutions," 3rd ed., Reinhold, New York, N.Y. 1958.

(8) R. L. Jones, *J. Lipid Res.*, **13**, 511 (1972).
(9) S. K. Perera and L. R. Fedor, *J. Am. Chem. Soc.*, **101**, 7390 (1979).
(10) D. J. Hupe, M. C. R. Kendall, G. T. Simner, and T. A. Spencer, *J. Am. Chem. Soc.*, **95**(7), 2260 (1973).
(11) R. L. Schowen, *Prog. Phys. Org. Chem.*, **9**, 275 (1972).
(12) R. M. Izatt and J. J. Christensen, in "Handbook of Biochemistry and Molecular Biology," Vol. I, 3rd ed., G. D. Fasman, Ed., CRC Press, Cleveland, Ohio, p. 151 ff.

ACKNOWLEDGMENTS

The authors thank Dr. Roy Bible and Mr. Arthur Ferreri for NMR studies and Ms. Lynelle Sachen for technical assistance.

α,α-Diphenylsuccinimide: Evaluation of Anticonvulsant and Hydrophobic Properties

GARY L. JONES **, ROBERT J. AMATO, and MARY F. JONES

Received December 13, 1982, from the *Department of Pathology, Texas College of Osteopathic Medicine, Fort Worth, TX 76107.* Accepted for publication January 13, 1983. *Present address: Physiology Department, University of Utah, Salt Lake City, UT 84117.

Abstract □ The anticonvulsant potencies (ED_{50}) of α,α-diphenylsuccinimide, phenytoin, and phenobarbital were evaluated in mice by a standard maximal electroshock technique. Potencies were expressed in terms of intraperitoneal dosage and blood and brain concentrations. Overt neurotoxicity (TD_{50}) was assessed by the rotorod method. These data were compared with relative hydrophobicities for the above compounds and three others [carbamazepine, cyheptamide, and (diphenylacetyl)urea] taken from the literature. An approximate parabolic dependence of anticonvulsant potency on hydrophobicity was observed regardless of the means of expressing potency (intraperitoneal dosage, blood concentration, or brain concentration); approximate optimal hydrophobicities were in the range of 2.18–2.23 (log P). Calculated therapeutic indices (TD_{50}/ED_{50}) also displayed a parabolic dependence on hydrophobicity, while toxic potency (TD_{50}) displayed a linear dependence (within the limited range of log P values studied). Implications of the parabolic dependence of anticonvulsant potency and linear dependence of toxic potency on hydrophobicity are discussed with respect to the possible mechanisms involved.

Keyphrases □ α,α-Diphenylsuccinimide—anticonvulsant potency, hydrophobic properties, overt neurotoxicity, maximal electroshock screen in mice □ Anticonvulsants—α,α-diphenylsuccinimide, hydrophobic properties, overt neurotoxicity, maximal electroshock screen in mice □ Hydrophobicity—α,α-diphenylsuccinimide, anticonvulsant potency, overt neurotoxicity, maximal electroshock screen in mice

The synthesis of α,α-diphenylsuccinimide (I) was reported by Miller and Long in 1951 (1). The anticonvulsant profile of the compound was evaluated in rats by a pentylenetetrazole model and in mice by a maximal electroshock (MES) model of epilepsy (1, 2). The compound was judged ineffective (500 mg/kg) in the prevention of pentylenetetrazole-induced seizures. However, sufficient dosage conferred complete protection against MES seizures; the ED_{50} (oral) in the MES model was 45 mg/kg (1, 2). A quantitative estimate of neurotoxicity was not provided. Since this early work, additional reports on the pharmacology of this compound have not appeared, and after three decades its profile remains unclear.

The present study was undertaken (*a*) to evaluate the anticonvulsant, neurotoxic, and hydrophobic properties of α,α-diphenylsuccinimide, phenytoin, and phenobarbital and (*b*) to compare these properties with the same properties for carbamazepine, cyheptamide, and (diphenylacetyl)urea (3, 4). Relative anticonvulsant potencies, determined using a standard MES model of epilepsy (5), are expressed in terms of intraperitoneal dose and blood and brain concentrations. Neurotoxicity was assessed using a rotorod method (6). Relative neurotoxicities and therapeutic indices are reported on the basis of intraperitoneal dose. Relative hydrophobicities were approximated using hydrophobic π-constants (7). Inspection of the data suggests that the potency of α,α-diphenylsuccinimide is subject to the same parabolic dependence on hydrophobicity already described for other compounds (8).

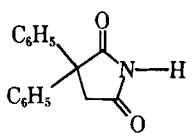

I

EXPERIMENTAL

Drugs—Phenytoin sodium[1] and phenobarbital sodium[2] were gifts. α,α-Diphenylsuccinimide was prepared utilizing a modification of a method described previously (1). The procedure involved the addition of ethyl bromoacetate to a mixture of diphenylacetonitrile in sodium ethoxide. The intermediate ethyl β-cyano-β,β-diphenylpropionate was hydrolyzed, initially in potassium hydroxide to β-cyano-β,β-diphenylpropionic acid and subsequently in concentrated hydrochloric acid to α,α-diphenylsuccinic acid. At this point the synthesis deviated from the published procedure. α,α-Diphenylsuccinic acid was heated at reflux in acetyl chloride to give the anhydride, an ethereal solution of which was treated with ammonia. The intermediate α,α-diphenylsuccinamic acid was removed by filtration and heated at reflux with acetyl chloride to give α,α-diphenylsuccinimide, which was recrystallized from methyl alcohol, mp 140–142°C (reported mp (1) 140–142°C). This material showed one spot on TLC (silica gel, alumina; chloroform). IR (chloroform): 1770 and 1740 cm^{-1} (5-membered ring, imide C=O's); ^1H-NMR (deuterochloroform): δ 3.38 (s, 2, CH_2), 7.16 (s, 10, ArH), and 8.84 ppm (s, 1, NH).

Animal Studies—Phenytoin sodium was suspended in 30% polyethylene glycol 400, and α,α-diphenylsuccinimide was suspended in 5% gum acacia. Phenobarbital sodium was dissolved in 0.9% NaCl. The suspensions were sonicated (probe-type) for ~5 min to produce a fine suspension. The drugs were administered intraperitoneally in a volume of 0.01 mL/g of body weight to male CF_1 mice[3], average weight 22 g. The mice, 30–32 d of age when received, were allowed several days to acclimatize before testing. Food and water were given *ad libitum*.

The anticonvulsant activity of each drug was evaluated by a standard MES test (5). A 60-Hz alternating current (50 mA) was applied for 0.2 s *via* corneal electrodes. Protection was defined as the absence of tonic

[1] Warner-Lambert Co., Morris Plains, N.J.
[2] Sterling-Winthrop Research Institute, New York, N.Y.
[3] Charles River Breeding Laboratories, Wilmington, Mass.

0022-3549/84/0300-0310$01.00/0